Available online at www.sciencedirect.com

ScienceDirect

Procedia CIRP 94 (2020) 41–45

www.elsevier.com/locate/procedia

11th CIRP Conference on Photonic Technologies [LANE 2020] on September 7-10, 2020

Effect of nanoparticle additivation on the microstructure and microhardness of oxide dispersion strengthened steels produced by laser powder bed fusion and directed energy deposition

C. Doñate-Buendia[a], R. Streubel[a], P. Kürnsteiner[b], M. B. Wilms[c], F. Stern[d], J. Tenkamp[d], E.Bruder[e], S. Barcikowski[a], B. Gault[b], K. Durst[e], J. H. Schleifenbaum[c], F. Walther[d], B. Gökce[a,*]

[a]*Technical Chemistry I and Center for Nanointegration Duisburg-Essen (CENIDE), University of Duisburg-Essen, 45141 Essen, Germany*
[b]*Department Microstructure Physics and Alloy Design, Max-Planck-Institut für Eisenforschung GmbH, 40237 Düsseldorf, Germany*
[c]*Chair for Digital Additive Production, RWTH Aachen University and Fraunhofer Institute of Laser Technology, 52074 Aachen, Germany*
[d]*Department of Materials Test Engineering, TU Dortmund University, 44227 Dortmund, Germany*
[e]*Physical Metallurgy, Materials Science Department, Technische Universität Darmstadt, 64287 Darmstadt, Germany*

* Corresponding author. Tel.: +49-201-183-3146; fax: +49-201-183-3049. E-mail address: bilal.goekce@uni-due.de

Abstract

In this contribution, the effect of nanoparticle additivation on the microstructure and microhardness of oxide dispersion strengthened steels (ODS) manufactured by laser powder bed fusion (L-PBF) and directed energy deposition (DED) additive manufacturing (AM) is studied. The powder composites are made of micrometer-sized iron-chromium-alloy based powder which are homogenously decorated with Y_2O_3 nanoparticles synthesized by pulsed laser fragmentation in water. Consolidated by L-PBF and DED, an enhanced microhardness of the AM-built ODS sample is found. This increase is related to the significant microstructural differences found between the differently processed samples.

Keywords: Oxide dispersion strengthened steel, ODS, Powder modification, Laser based powder bed fusion, Directed energy deposition, Laser metal deposition, Nanoparticles

1. Introduction

The manufacturing of steel components represents a pillar of the industrial development due to their high demand in fundamental areas like construction, automation or aeronautics [1,2]. In that sense, the aim to develop steel parts with complex geometries and specific properties requires the development and employment of different manufacturing technologies. Powder and laser based additive manufacturing (powder LAM) englobes the techniques based on the processing of powders by high power lasers to manufacture the final pieces based on the melting and solidification of the base material [3]. The flexibility of the technique for the employment of a wide library of base materials relies on the possibility of optimizing the laser and processing parameters for each specific material [4]. The scanning methodology and the layer by layer deposit and growth procedure leads to an enhanced versatility when complex geometries are desired [5]. Inside the general term powder LAM, two main technologies can be highlighted due to their standard use in metal powders processing, i.e. directed energy deposition (DED) and laser powder bed fusion (L-PBF). While both are based on the same general principle, their differences rely on the depositing methodology of the powder material, which can affect the dynamics of the process [6]. Both techniques are conventionally applied in the processing of metallic powders. Consequently, their comparison is necessary to select the optimum technique for all individual processing conditions.

10.1016/j.procir.2020.09.009

There exist a wide library of processable powders, even more, if modifications for enhanced performance are taken into account [7]. In this context, the controlled addition of oxide nanoparticles to the steel powders has been proved to modify the properties of the generated steel pieces, giving rise to oxide dispersion strengthened (ODS) steels [8]. Yttrium based oxides have been extensively employed in the modification of steel powders due to their proven mechanical reinforcement [9] and radiation sink effect [10]. Generally, due to their lattice mismatch with the metal matrix they act as dispersoids, hindering dislocation propagation and acting as sinks for radiation-induced defects [11]. The most common route for their fabrication is reactive ball milling and annealing [12,13]. Nevertheless, achieving control over nanoparticle dispersion and size is important as it influences the performance of the final pieces [14]. Consequently, a fabrication route based on the synthesis of colloidal nanoparticles by laser fragmentation in liquids (LFL), followed by their pH-controlled dielectrophoretic supporting on the steel powder has been proposed for an enhanced control of the nanoparticle dispersion and size evolution during the different steps towards the development of ODS steel samples [15–17].

In the present study, the achieved control over nanoparticle features during the processing steps for ODS steel preparation by the LFL synthesis route is explored. To do so, the nanoparticle size, dispersion, and composition is analyzed after fragmentation, supporting on the steel micro-powder and processing by DED and L-PBF. This way, nanoparticle evolution during the complete additive manufacturing process of an ODS steel sample is monitored for a better understanding of the influence of each technique over the nanoparticle distribution, microstructure of the fabricated piece, and hence over the ODS steel final properties.

2. Materials and methods

The materials employed for the ODS steel manufacture by DED and L-PBF are Y_2O_3 nanoparticles and a PM2000 ferritic steel powder. The raw Y_2O_3 nanoparticles are commercially acquired from Sigma Aldrich and dispersed in ultrapure deionized water (pH adjusted to 3.5 for stability) for deagglomeration and size reduction by laser fragmentation in liquids (LFL) employing an f = 100 mm cylindrical lens, Fig. 1 top part [18]. This technique offers numerous advantages for the preparation of colloidal nanomaterials as it yields a wide library of processable materials [19–21], reduced waste generation and high nanoparticle output [22,23]. The supporting of the generated nanoparticles on the steel powder is achieved by the addition of the PM2000 to the colloidal Y_2O_3 nanoparticles and the modification of the pH to a value between the isoelectric point of both materials, Fig. 1 bottom part, by NaOH addition [24].

The prepared powder material is then processed by DED and L-PBF, respectively. In the first case, Fig. 2a, the powder is directly sent to the laser beam by a nozzle, the interaction with the high power laser beam melts it and gets the powder material deposited on the workpiece.

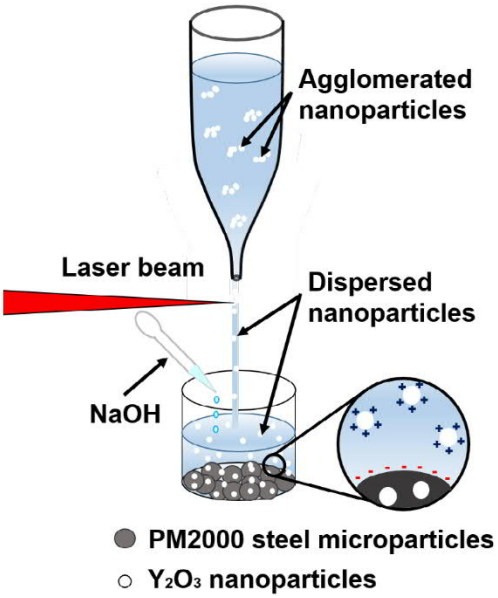

Fig. 1. Schematic illustration of the passage reactor LFL setup and dielectrophoretic nanoparticle adsorption on the steel powder by pH control.

Then the material solidifies, obtaining the final ODS steel samples and controlling the sample geometry by a scanning system. In the case of the L-PBF, Fig. 2b, the powder is spread over a substrate and the laser beam controlled by a scanning system melts the interacting areas. Again, the melted material solidifies forming the ODS steel sample. The non-irradiated powder material can be removed and reutilized.

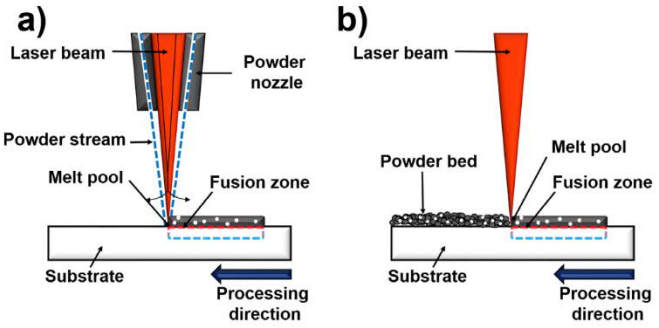

Fig. 2. Representative scheme of the (a) DED and (b) L-PBF laser additive manufacturing technologies.

Different analytical techniques are employed to characterize the nanoparticle size at the different stages of the process as well as their dispersion. After LFL, transmission electron microscopy (TEM) measurements are performed to evaluate the nanoparticle size, Fig. 3a. When the Y_2O_3 nanoparticles are supported on the steel powder, scanning electron microscopy (SEM) images are acquired to visualize nanoparticle size and dispersion on the surface of the steel powder, Fig. 3b. It should be noted that SEM is needed to visualize the nanoparticles on the steel surface, however, the spatial resolution achievable is lower than TEM and small nanoparticles may not appear. Finally, after processing the samples by DED and L-PBF, are analyzed by SEM-energy dispersive X-ray spectroscopy (EDS) and electron backscatter diffraction (EBSD). Microhardness measurements (HV0.1) are conducted with an applied load of

0.9807 N. The mean hardness is calculated by performing at least five indents.

3. Results and discussion

The evolution of the nanoparticles during LAM processing is compared from the Y_2O_3 nanoparticles synthesized by LFL. The TEM image in Fig. 3a displays that a bimodal distribution is found, a smaller population of 3.2 ± 0.6 nm and larger particles with a 28 ± 8 nm size distribution. The presence of two differentiated particle populations is potentially beneficial to observe the effect of the manufacturing process for both nanoparticle sizes. Besides, nanoparticle size is reported to influence the strengthening mechanism in ODS steels [25]. In particular, for small particles, dislocation cutting is the predominant effect, while for larger ones dislocation looping around the particle is the main strengthening mechanism [26].

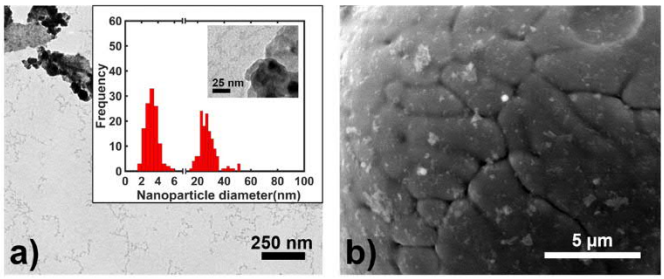

Fig. 3. (a) Y_2O_3 nanoparticle size distribution after LFL measured by TEM. (b) Dispersion and size of the Y_2O_3 nanoparticles supported on PM2000 powder by electrostatic deposition.

After deposition of the nanoparticles on the PM2000 steel powder, the SEM image, Fig. 3b, demonstrates a fine dispersion on the surface with the addition of only a 0.08 wt% of Y_2O_3 nanoparticles. It should be noted that SEM images are limited by the spatial resolution of the technique, and so smaller nanoparticles could be present in the steel surface, lowering the average nanoparticle size and reducing the interparticle distance.

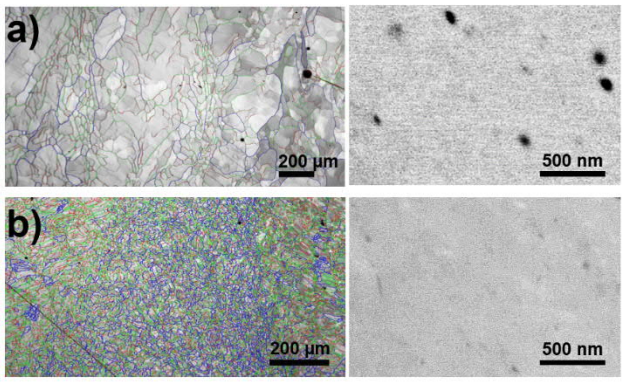

Fig. 4. Image quality (band contrast) maps with superimposed grain boundaries (misorientation: 2-5° green, 5-15° red, >15° blue), left, detailed view of nanoinclusions, right (backscatter electron micrograph), of the ODS steel pieces manufactured by (a) DED and (b) L-PBF.

After parts were printed with the nano-decorated powder by DED and L-PBF, the distribution and size of the resulting nanoinclusions are characterized by SEM and EBSD, Fig. 4.

The manufacturing method is shown to influence the grain size, which is known to have a fundamental impact on the mechanical properties of the metal [25,26]. It is visible that the grain size is significantly bigger in the DED sample, Fig. 4a, than in the L-PBF sample, Fig. 4b. The differences are attributed to the higher cooling rate in L-PBF and suggest a superior mechanical strength of the L-PBF sample due to the smaller grain size [27]. Besides, higher magnification images of the samples show the presence of larger particles in the DED piece. To investigate which elements might be contained in these particles, EDS analysis is performed, Fig. 5.

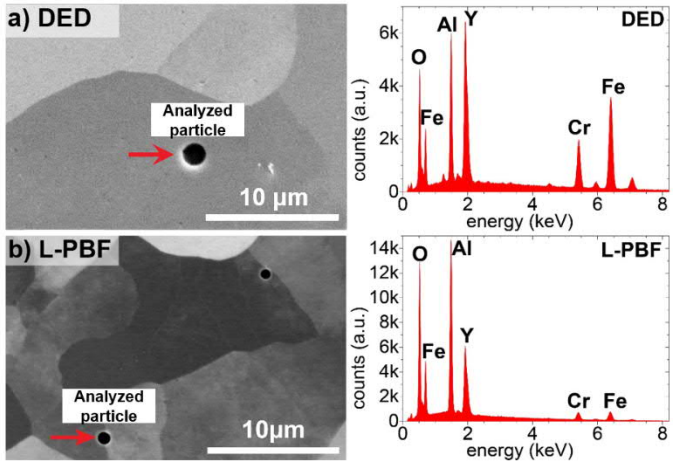

Fig. 5. Backscatter electron SEM images of the nanoinclusions, left, and EDS analysis of the particles marked by the arrow, right, of the ODS steel pieces manufactured by (a) DED and (b) L-PBF. Note that the spectrum is not exclusively from the particle itself but might contain some contribution from the matrix as the excitation volume in SEM-EDS might be larger than the particle.

The measurements reveal the presence of Y, O and Al in the particle and its surrounding, Fig. 5a and Fig. 5b. This result, together with the differences in particle size observed in Fig. 4, suggests that stronger agglomeration and particle size growing of the initial Y_2O_3 nanoparticles occurs during DED manufacturing, while these effects are reduced by L-PBF processing. The presence of Al in both samples is associated to its precipitation during processing.

Microhardness measurements (HV0.1) of the cross-sections show different hardness values depending on the processing route. The results are given in Table 1. As evident, processing with L-PBF results in a slightly higher hardness compared to DED. A possible explanation for this variation can be found in the higher cooling rates in L-PBF resulting in a finer microstructure compared to the DED [28] process as can be seen in Fig. 4a) and b), thus, causing differing hardness values. Additionally, the larger size of nanoinclusions as shown in Fig. 4a) in the DED steel specimens leads to a potentially lower effect of dispersion strengthening. However, the amount of nanoinclusions inherited in the steel is considerably low so that a considerable influence of the dispersion strengthening on the measured microhardness is not to be expected, especially at

room temperature [29]. Nevertheless, it is expected that a significant difference in terms of material strength at high temperatures due to the two processing routes will be identifiable.

Table 1. Microhardness (HV0.1) of the DED and L-PBF samples

Microhardness	**DED**	**L-PBF**
HV0.1	223 ± 9	247 ± 8

4. Conclusions

A study of the evolution and effect of nanoparticles in powder LAM of an ODS steel has been performed. The influence of the processing technique has been studied by comparing the microstructure and composition of DED with L-PBF manufactured parts. Regarding the microstructure, L-PBF processing is shown to reduce the grain size and increase grain boundaries compared to DED, which is expected to result in an enhanced strengthening of the built parts.

Concerning the evolution of the initially added 0.08 wt% Y_2O_3 nanoparticles, a fine dispersion is achieved on the steel powder decoration process by electrostatic deposition. After processing, an enrichment of Y, O and Al in the particles and its surrounding is shown by EDS analysis. The composition analysis together with SEM visualization of the nanoinclusions indicates that L-PBF is reducing agglomeration of the Y_2O_3 particles. During DED processing, apparently agglomeration of the nanoparticles is taking place. Since a fine dispersion and small nanoparticles are desired to enhance the strengthening effect due to the Orowan mechanism, L-PBF is potentially a more suitable technique compared to DED for the manufacturing of ODS steels from Y_2O_3 nanoparticle decorated PM2000 powder.

Acknowledgements

The authors acknowledge the funding by the Deutsche Forschungsgemeinschaft (DFG, German Research Foundation) within the priority program (SPP) 2122 “Materials for Additive Manufacturing” and within the CRC/TRR 270 Project-ID 405553726.

References

[1] N.R. Baddoo, Stainless steel in construction: A review of research, applications, challenges and opportunities, J. Constr. Steel Res. 64 (2008) 1199–1206. https://doi.org/10.1016/j.jcsr.2008.07.011.

[2] Y. Inoue, M. Kikuchi, Present and Future Trends of Stainless Steel for Automotive Exhaust System, 2003.

[3] D.D. Gu, W. Meiners, K. Wissenbach, R. Poprawe, Laser additive manufacturing of metallic components: Materials, processes and mechanisms, Int. Mater. Rev. 57 (2012) 133–164. https://doi.org/10.1179/1743280411Y.0000000014.

[4] N. Shamsaei, A. Yadollahi, L. Bian, S.M. Thompson, An overview of Direct Laser Deposition for additive manufacturing; Part II: Mechanical behavior, process parameter optimization and control, Addit. Manuf. 8 (2015) 12–35. https://doi.org/10.1016/j.addma.2015.07.002.

[5] M. Alkhayat, E. Khavkin, A. Gasser, W. Meiners, I. Kelbassa, Comparison of geometrical properties of parts manufactured by powder bed based (SLM) and powder fed based (LMD) laser additive manufacturing technologies, in: Int. Congr. Appl. Lasers Electro-Optics, Laser Institute of America, 2018: pp. 740–745. https://doi.org/10.2351/1.5063125.

[6] S. Li, H. Xiao, K. Liu, W. Xiao, Y. Li, X. Han, J. Mazumder, L. Song, Melt-pool motion, temperature variation and dendritic morphology of Inconel 718 during pulsed- and continuous-wave laser additive manufacturing: A comparative study, Mater. Des. 119 (2017) 351–360. https://doi.org/10.1016/J.MATDES.2017.01.065.

[7] B.M. Arkhurst, J.-J. Park, C.-H. Lee, J.H. Kim, Direct Laser Deposition of 14Cr Oxide Dispersion Strengthened Steel Powders Using Y2O3 and HfO2 Dispersoids, Korean J. Met. Mater. 55 (2017) 550–558. https://doi.org/10.3365/KJMM.2017.55.8.550.

[8] M. Brocq, B. Radiguet, S. Poissonnet, F. Cuvilly, P. Pareige, F. Legendre, Nanoscale characterization and formation mechanism of nanoclusters in an ODS steel elaborated by reactive-inspired ball-milling and annealing, J. Nucl. Mater. 409 (2011) 80–85. https://doi.org/10.1016/J.JNUCMAT.2010.09.011.

[9] J.S. Benjamin, Dispersion strengthened superalloys by mechanical alloying, 1 (1970) 2943–2951. https://doi.org/10.1007/BF03037835.

[10] V.V. Sagaradze, V.I. Shalaev, V.L. Arbuzov, B.N. Goshchitskii, Y. Tian, W. Qun, S. Jiguang, Radiation resistance and thermal creep of ODS ferritic steels, J. Nucl. Mater. 295 (2001) 265–272. https://doi.org/10.1016/S0022-3115(01)00511-6.

[11] K.E. Knipling, B.W. Baker, D.K. Schreiber, Mechanisms of Particle Coarsening and Phase Transformation in Oxide Dispersion Strengthened Steels During Friction Stir Welding, in: Proceeding Microsc. Microanal., 2016: pp. 676–677.

[12] B. AlMangour, D. Grzesiak, J.-M. Yang, Selective laser melting of TiB2/H13 steel nanocomposites: Influence of hot isostatic pressing post-treatment, J. Mater. Process. Technol. 244 (2017) 344–353. https://doi.org/10.1016/J.JMATPROTEC.2017.01.019.

[13] B. AlMangour, D. Grzesiak, J.-M. Yang, Nanocrystalline TiC-reinforced H13 steel matrix nanocomposites fabricated by selective laser melting, Mater. Des. 96 (2016) 150–161. https://doi.org/10.1016/J.MATDES.2016.02.022.

[14] H.J. Chang, H.Y. Cho, J.H. Kim, Stability of Y-Ti-O nanoparticles during laser melting of advanced oxide dispersion-strengthened steel powder, J. Alloys Compd. 653 (2015) 528–533. https://doi.org/10.1016/j.jallcom.2015.08.273.

[15] R. Streubel, M.B. Wilms, C. Doñate-Buendía, A. Weisheit, S. Barcikowski, J.H. Schleifenbaum, B. Gökce, Depositing laser-generated nanoparticles on powders for additive manufacturing of oxide dispersed strengthened alloy parts via laser metal deposition, Jpn. J. Appl. Phys. (2018). https://doi.org/10.7567/JJAP.57.040310.

[16] C. Doñate-Buendía, F. Frömel, M.B. Wilms, R. Streubel, J. Tenkamp, T. Hupfeld, M. Nachev, E. Gökce, A. Weisheit, S. Barcikowski, F. Walther, J.H. Schleifenbaum, B. Gökce, Oxide dispersion-strengthened alloys generated by laser metal deposition of laser-generated nanoparticle-metal powder composites, Mater. Des. 154 (2018) 360–369. https://doi.org/10.1016/j.matdes.2018.05.044.

[17] M.B. Wilms, R. Streubel, F. Frömel, A. Weisheit, J. Tenkamp, F. Walther, S. Barcikowski, J.H. Schleifenbaum, B. Gökce, Laser additive manufacturing of oxide dispersion strengthened steels using laser-generated nanoparticle-metal composite powders,

Procedia CIRP. 74 (2018) 196–200. https://doi.org/10.1016/J.PROCIR.2018.08.093.

[18] P. Wagener, S. Barcikowski, Laser fragmentation of organic microparticles into colloidal nanoparticles in a free liquid jet, Appl. Phys. A. 101 (2010) 435–439. https://doi.org/10.1007/s00339-010-5814-x.

[19] T. Schmitz, U. Wiedwald, C. Dubs, B. Gökce, Ultrasmall Yttrium Iron Garnet Nanoparticles with High Coercivity at Low Temperature Synthesized by Laser Ablation and Fragmentation of Pressed Powders, ChemPhysChem. 18 (2017) 1125–1132. https://doi.org/10.1002/cphc.201601183.

[20] C. Doñate-Buendia, R. Torres-Mendieta, A. Pyatenko, E. Falomir, M. Fernández-Alonso, G. Mínguez-Vega, Fabrication by Laser Irradiation in a Continuous Flow Jet of Carbon Quantum Dots for Fluorescence Imaging, ACS Omega. 3 (2018) 2735–2742. https://doi.org/10.1021/acsomega.7b02082.

[21] D. Zhang, Z. Ma, M. Spasova, A.E. Yelsukova, S. Lu, M. Farle, U. Wiedwald, B. Gökce, Formation Mechanism of Laser-Synthesized Iron-Manganese Alloy Nanoparticles, Manganese Oxide Nanosheets and Nanofibers, Part. Part. Syst. Charact. 34 (2017) 1600225. https://doi.org/10.1002/ppsc.201600225.

[22] T. Hupfeld, T. Laumer, T. Stichel, T. Schuffenhauer, J. Heberle, S. Barcikowski, B. Gökce, A new approach to coat PA12 powders with laser-generated nanoparticles for selective laser sintering, Procedia CIRP. 74 (2018) 244–248. https://doi.org/10.1016/J.PROCIR.2018.08.103.

[23] S. Kohsakowski, A. Santagata, M. Dell'Aglio, A. de Giacomo, S. Barcikowski, P. Wagener, B. Gökce, High productive and continuous nanoparticle fabrication by laser ablation of a wire-target in a liquid jet, Appl. Surf. Sci. 403 (2017) 487–499. https://doi.org/10.1016/J.APSUSC.2017.01.077.

[24] G. Marzun, C. Streich, S. Jendrzej, S. Barcikowski, P. Wagener, Adsorption of Colloidal Platinum Nanoparticles to Supports: Charge Transfer and Effects of Electrostatic and Steric Interactions, Langmuir. 30 (2014) 11928–11936. https://doi.org/10.1021/la502588g.

[25] M. Ratti, D. Leuvrey, M.H. Mathon, Y. de Carlan, Influence of titanium on nano-cluster (Y, Ti, O) stability in ODS ferritic materials, J. Nucl. Mater. 386–388 (2009) 540–543. https://doi.org/10.1016/J.JNUCMAT.2008.12.171.

[26] M.N. SHETTY, Dislocations and Mechanical Behaviour of Materials, 2013.

[27] A. Lasalmonie, J.L. Strudel, Influence of grain size on the mechanical behaviour of some high strength materials, J. Mater. Sci. 21 (1986) 1837–1852. https://doi.org/10.1007/BF00547918.

[28] D. Herzog, V. Seyda, E. Wycisk, C. Emmelmann, Additive manufacturing of metals, Acta Mater. 117 (2016) 371–392. https://doi.org/10.1016/j.actamat.2016.07.019.

[29] I. Bogachev, A. Yudin, E. Grigoryev, I. Chernov, M. Staltsov, O. Khasanov, E. Olevsky, Microstructure Investigation of 13Cr-2Mo ODS Steel Components Obtained by High Voltage Electric Discharge Compaction Technique, Materials (Basel). 8 (2015) 7342–7353. https://doi.org/10.3390/ma8115381.